



OPEN

Children develop robust and sustained cross-reactive spike-specific immune responses to SARS-CoV-2 infection

Alexander C. Dowell¹, Megan S. Butler^{1,15}, Elizabeth Jinks^{1,15}, Gokhan Tut^{1,15}, Tara Lancaster¹, Panagiota Sylla¹, Jusnara Begum¹, Rachel Bruton¹, Hayden Pearce¹, Kriti Verma¹, Nicola Logan², Grace Tyson², Eliska Spalkova¹, Sandra Margielewska-Davies¹, Graham S. Taylor¹, Eleni Syrimi¹, Frances Baawuah³, Joanne Beckmann⁴, Ifeanyichukwu O. Okike^{3,5}, Shazaad Ahmad⁶, Joanna Garstang^{7,8}, Andrew J. Brent^{9,10}, Bernadette Brent⁹, Georgina Ireland³, Felicity Aiano³, Zahin Amin-Chowdhury³, Samuel Jones³, Ray Borrow¹¹, Ezra Linley¹¹, John Wright¹², Rafaq Azad¹², Dagmar Waiblinger¹², Chris Davis², Emma C. Thomson², Massimo Palmarini², Brian J. Willett², Wendy S. Barclay¹³, John Poh³, Gayatri Amirthalingam³, Kevin E. Brown³, Mary E. Ramsay³, Jianmin Zuo¹, Paul Moss^{1,16} and Shamez Ladhani^{3,14,16}

SARS-CoV-2 infection is generally mild or asymptomatic in children but a biological basis for this outcome is unclear. Here we compare antibody and cellular immunity in children (aged 3–11 years) and adults. Antibody responses against spike protein were high in children and seroconversion boosted responses against seasonal Beta-coronaviruses through cross-recognition of the S2 domain. Neutralization of viral variants was comparable between children and adults. Spike-specific T cell responses were more than twice as high in children and were also detected in many seronegative children, indicating pre-existing cross-reactive responses to seasonal coronaviruses. Importantly, children retained antibody and cellular responses 6 months after infection, whereas relative waning occurred in adults. Spike-specific responses were also broadly stable beyond 12 months. Therefore, children generate robust, cross-reactive and sustained immune responses to SARS-CoV-2 with focused specificity for the spike protein. These findings provide insight into the relative clinical protection that occurs in most children and might help to guide the design of pediatric vaccination regimens.

The SARS-CoV-2 pandemic has resulted in over 4.2 million deaths so far and the most notable determinant of outcome is age at the time of primary infection¹. SARS-CoV-2 infection in children is generally asymptomatic or mild and contrasts with high rates of hospitalization and death in older adults². As such, there is interest in understanding the profile of the immune response to SARS-CoV-2 in children. Such studies are limited to date but have reported reduced magnitude of both antibody and cellular responses in comparison to adults and an absence of nucleocapsid-specific antibody responses during or early postinfection^{3–6}. One unique feature of SARS-CoV-2 infection in children is the development of a rare complication known as pediatric inflammatory multisystem syndrome temporally associated with SARS-CoV-2 (PIMS-TS), also known as multisystem inflammatory syndrome in children (MIS-C), which shares features with Kawasaki disease and toxic shock syndrome^{7,8}. MIS-C develops approximately

2–4 weeks after infection in children with a median age of 9 years⁹. The immunological basis for this condition is unclear but it is characterized by diffuse endothelial involvement and broad autoantibody production¹⁰.

One potential determinant of differential immune responses to SARS-CoV-2 across the life course may be the timing of exposure to the four additional endemic human coronaviruses (hCoVs). These comprise the Beta-coronaviruses OC43 and HKU-1, which have 38% and 35% amino acid homology with SARS-CoV-2, and the more distantly related Alpha-coronaviruses NL63 and 229E, each with around 31% homology¹¹. These coronaviruses cause frequent mild childhood infections and antibody seroconversion occurs typically before the age of 5 years. Infection with one of the Alpha- or Beta-coronaviruses provides short-term immunity against reinfection from coronaviruses and represents transient cross-reactive immunity within the subtypes^{12–14}. As such, recent hCoV infection

¹Institute of Immunology & Immunotherapy, College of Medical and Dental Sciences, University of Birmingham, Birmingham, UK. ²MRC-University of Glasgow Centre for Virus Research, Glasgow, UK. ³Public Health England, 61 Colindale Avenue, London, UK. ⁴East London NHS Foundation Trust, London, UK. ⁵University Hospitals of Derby and Burton NHS Foundation Trust, Derby, UK. ⁶Manchester University NHS Foundation Trust, Manchester, UK. ⁷Birmingham Community Healthcare NHS Trust, Aston, UK. ⁸Institute of Applied Health Research, College of Medical and Dental Sciences, University of Birmingham, Birmingham, UK. ⁹Oxford University Hospitals NHS Foundation Trust, Oxford, UK. ¹⁰University of Oxford, Wellington Square, Oxford, UK. ¹¹Public Health England, Manchester Royal Infirmary, Manchester, UK. ¹²Bradford Institute for Health Research, Bradford Teaching Hospitals NHS Foundation Trust, Bradford, UK. ¹³Department of Infectious Disease, Imperial College, London, UK. ¹⁴Paediatric Infectious Diseases Research Group, St. George's University of London, London, UK. ¹⁵These authors contributed equally: Megan S. Butler, Elizabeth Jinks, Gokhan Tut. ¹⁶These authors contributed equally: Paul Moss, Shamez Ladhani. ✉e-mail: p.moss@bham.ac.uk

might presensitize children against SARS-CoV-2 infection and may explain cross-reactive SARS-CoV-2-neutralizing antibodies in some seronegative children¹⁵. Immune responses against hCoV are retained throughout life but do not provide sterilizing immunity¹³. Consequently, recurrent infections are common, generating concern that a similar pattern will be observed after SARS-CoV-2 infection.

COVID-19 vaccines are now being administered widely to adult populations and are also being delivered to children in some countries. Therefore, it is imperative to understand the profile of SARS-CoV-2-specific immune responses in children after natural infection to inform vaccination strategy. In this study, we provide a comprehensive characterization of the convalescent humoral and cellular immune response in a cohort of 91 primary school-aged children compared with 154 adults taking part in the COVID-19 surveillance in school KIDs (sKIDs) study¹⁶. We demonstrate a markedly different profile of immune response after SARS-CoV-2 infection in children compared to adults. These findings have potential implications for understanding protective or pathological immune responses to infection in children and might help to guide and interpret COVID-19 vaccination regimens for children.

Results

Children develop robust antibody responses to SARS-CoV-2. Blood samples were obtained from 91 children and 154 adults, including 35 children and 81 adults known to be seropositive in previous rounds of testing. All infections were asymptomatic or mild and no staff or students in the cohort required medical care or hospitalization. The median age of children was 7 years (range 3–11) while that of adults was 41 years (range 20–71). The SARS-CoV-2 antibody profile was assessed using the Meso Scale Discovery (MSD) V-PLEX serology platform to determine serological responses against spike, receptor binding domain (RBD), N-terminal domain (NTD) and nucleocapsid (N). In total, 47% of children and 59% of adults were seropositive (Supplementary Table 1). To ensure the sensitivity of our assays, we obtained convalescent plasma samples from 35 children with PCR-confirmed SARS-CoV-2. Thirty-four were seropositive in the assay while 1 donor mounted no detectable antibody response to any antigen tested. Prepandemic plasma samples from 9 children and 50 adults all gave negative results and demonstrated the specificity of the assay (Extended Data Fig. 1).

Seropositive children and adults demonstrated broadly similar antibody responses against viral proteins. However, geometric mean antibody titers against all four regions were higher in children, most notably against the NTD and RBD domains, which showed 2.3-fold and 1.7-fold increases, respectively, although these did not reach statistical significance (Fig. 1a). In contrast to previous reports³, we also observed antibody responses against nucleoprotein, with a 1.3-fold increased antibody titer compared to adults (Fig. 1a,b).

SARS-CoV-2 infection boosts hCoV binding antibodies in children. Pre-existing immune responses against seasonal coronaviruses might act to modulate clinical outcome after primary SARS-CoV-2 infection and cross-reactive neutralizing antibodies have been reported in SARS-CoV-2-seronegative children¹⁵. Consequently, we compared antibody levels against the four hCoVs in SARS-CoV-2 in seronegative and seropositive children and adults.

A 1.2–1.4-fold increase in the titer against hCoV was evident in SARS-CoV-2 seropositive adults compared to the seronegative group. In contrast, antibody levels against all 4 viruses were boosted markedly in SARS-CoV-2 seropositive children, with 2.3, 1.9, 1.5 and 2.1-fold higher antibody levels compared to the seronegative group. These were significant for OC43 and HKU-1 ($P=0.0071$ and $P=0.0024$ Brown–Forsythe and Welch’s analysis of variance (ANOVA), with Dunnett’s T3 multiple comparison test) (Fig. 2a). Notably, the level of hCoV-specific antibodies in seropositive

children was comparable to adults, whereas seronegative children possessed lower responses than adults (Supplementary Table 1).

To assess if this effect was specific to hCoV or represented a more general effect of SARS-CoV-2 infection on antibody responses against heterologous infection, we also examined antibody titers against influenza subtypes and respiratory syncytial virus in relation to SARS-CoV-2 serostatus. No change in antibody titer against these viruses was seen in either children or adults (Fig. 2b). These data show that SARS-CoV-2 infection in children specifically boosts humoral responses against hCoV.

SARS-CoV-2 antibodies in children cross-react with Beta-hCoV. Given the increase in hCoV-specific antibody titers after SARS-CoV-2 infection in children, we next assessed to what extent this was cross-reactive against SARS-CoV-2 or could represent an hCoV-specific response. As such, recombinant S1 or S2 domain protein from SARS-CoV-2 was used to preabsorb plasma samples before assessment of antibody levels to both SARS-CoV-2 and the four hCoV subtypes.

As expected, preabsorption with both the S1 and S2 domains markedly reduced antibody titers against total spike ($P<0.0001$ and $P=0.0024$, respectively, Friedman test with Dunn’s multiple comparisons test). The S1 domain, but not the S2 domain, absorbed RBD- and NTD-specific antibodies against SARS-CoV-2 while no influence was observed in relation to nucleocapsid-specific binding for either domain (Fig. 3). Of note, the S1 domain did not reduce antibody binding to any of the four hCoV subtypes, indicating little evidence for cross-reactive antibodies against this domain. The S2 domain, however, selectively reduced antibody binding to the two hCoV Beta-coronaviruses OC43 and HKU-1 ($P<0.0001$ and $P=0.0014$, respectively by one-way repeated measures ANOVA with Holm–Sidak’s multiple comparison test). No such effect was observed in relation to binding to the Alpha-coronaviruses NL63 and 229e (Fig. 3).

These data show that the S1 region is the immunodominant target of antibody responses in children. However, antibodies that are cross-reactive against Beta-coronavirus are largely specific for the S2 domain and contribute to the higher SARS-CoV-2-specific titer in children.

Children develop robust cellular immune responses to spike protein. We next assessed the magnitude and profile of the cellular immune response against SARS-CoV-2 in children and adults. Enzyme-linked immunosorbent spot (ELISpot) analysis against overlapping peptide pools from spike and a combination of nucleocapsid and membrane and envelope (nucleoprotein and viral membrane (N/M)) was performed on samples from 57 children and 93 adults, including 37 and 64 respectively who were seropositive.

As expected, ELISpot responses were common in SARS-CoV-2 seropositive donors with 89% (33 out of 37) of seropositive children and 80% (51 out of 64) of seropositive adults showing a positive ELISpot response to spike and/or the N/M pool.

The magnitude of the cellular response against spike was 2.1-fold higher in children, with median values of 533 spots per million compared to 195 in adults ($P=0.0003$, Brown–Forsythe and Welch’s ANOVA with Dunnett’s T3 multiple comparisons test) (Fig. 4a). Cellular responses against the N/M pool were relatively lower in children compared to spike such that the S:N/M ratio was markedly elevated in children at 4.7 compared to 1.8 in adults ($P=0.0007$, Brown–Forsythe and Welch’s ANOVA with Dunnett’s T3 multiple comparisons test) (Fig. 4b). Eighty-six percent of children showed a positive response to spike while only 43% responded to the N/M pool. Within adults these values were 70% and 63%, respectively (Fig. 4c).

The supernatant from ELISpot was analyzed using a multi-analyte bead assay to compare the profile of cytokine production by SARS-CoV-2-specific T cells from children and adults. Samples

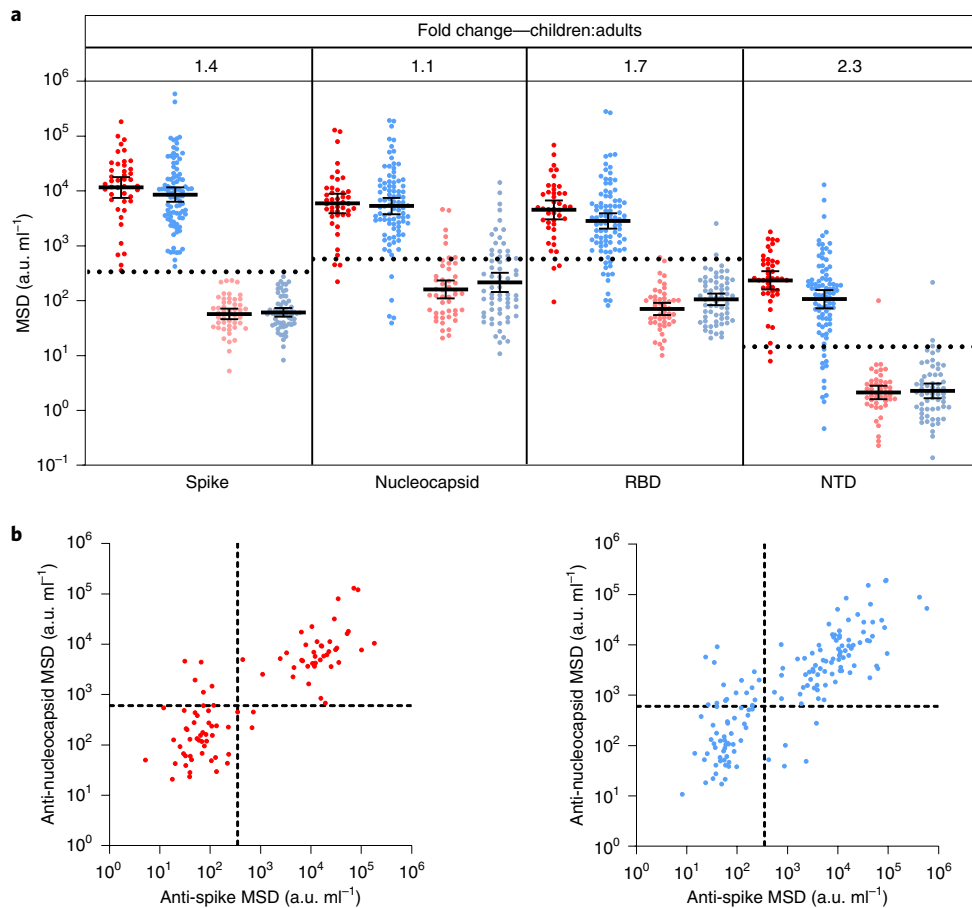


Fig. 1 | Children and adults develop coordinated antibody responses to SARS-CoV-2. a, SARS-CoV-2 antibody levels measured by MSD assay in children ($n=91$) and adults ($n=154$). Serostatus was assigned based on spike serology and used to divide the cohorts into seropositive (red/blue) and seronegative (light red/light blue) (seropositive/negative children $n=43/48$, adults $n=91/63$, respectively). The dotted lines represent cutoff values for serostatus. Fold change indicates the difference between the GMTs in seropositive children and adults. The bars indicate the geometric mean with 95% confidence interval (CI). **b**, The level of the spike- and nucleocapsid-specific antibody response was correlated within individual donors and revealed a coordinated response to both proteins. a.u., arbitrary unit.

from adult donors showed a marked interleukin-2 (IL-2) response with lower levels of interleukin-10 (IL-10) production. In contrast, IL-2 levels in samples from children were very low (Fig. 4d), indicating differential functional response compared to adults. Indeed, analysis of three children by flow cytometry indicated that CD8⁺IL-2-TNF⁺IFN- γ ⁺ T cells constituted the bulk of the spike-specific T cell response in children (Extended Data Fig. 2).

Notably, cellular responses were also observed in 60% (12 out of 20) of seronegative children, all of whom were seronegative by 3 different serology platforms. Cellular responses of variable but lower magnitude were also present in 34% (10 out of 29) of seronegative adults (Fig. 4a). Two children and one adult classed as seronegative had anti-nucleocapsid antibodies (Supplementary Table 2) but this was insufficient to provide definitive serostatus. These cellular responses in seronegative donors were markedly spike-specific, with elevated S:N/M ratios of 7.1 and 5 in children and adults, respectively (Fig. 4b), indicating pre-existing cross-reactive immunity. Indeed seronegative children (7 out of 12) and seronegative adults (6 out of 10) with a positive ELISpot demonstrated high antibody levels to 1 or more hCoV (Supplementary Table 2), potentially indicating recent hCoV infection.

To examine the presence of cross-reactive T cells in seronegative children, we hypothesized that expansion of T cells in response to SARS-CoV-2 would be associated with an increase in hCoV-reactive responses. As such we first stimulated cells from SARS-CoV-2

seronegative donors with SARS-CoV-2 peptides and then assessed the response to peptides from SARS-CoV-2 and also peptide pools from the Alpha and Beta hCoVs. Markedly increased cellular responses to both Alpha and Beta hCoVs were seen after culture (8.6-fold and 8.9-fold, respectively) (Fig. 4e), indicating SARS-CoV-2-driven expansion of broadly cross-reactive T cells. Finally, to definitively assess the presence of cross-reactive T cells in children, we obtained pre-pandemic PBMCs from children and observed that 50% of these had notable responses to spike by ELISpot but lacked cellular responses against N/M peptides (Fig. 4f). Matched plasma samples, available for three donors, showed that antibody responses against HKU-1 and 229E were twofold and fivefold greater in a donor with high cellular responses compared to two children who lacked cellular responses.

Overall these data show that cross-reactive coronavirus-specific T cell responses are present within a high proportion of children.

Children maintain SARS-CoV-2-specific immune responses for 12 months. We next assessed the longevity of immune responses within a subgroup of 35 children and 81 adults who had seroconverted at least 6 months before the analysis. All children retained humoral immunity while 7% (6/81) of previously seropositive adults failed to show antibody responses. Children also maintained higher antibody titers against spike and RBD, which were 1.8-fold higher than adults (Fig. 5a,b).

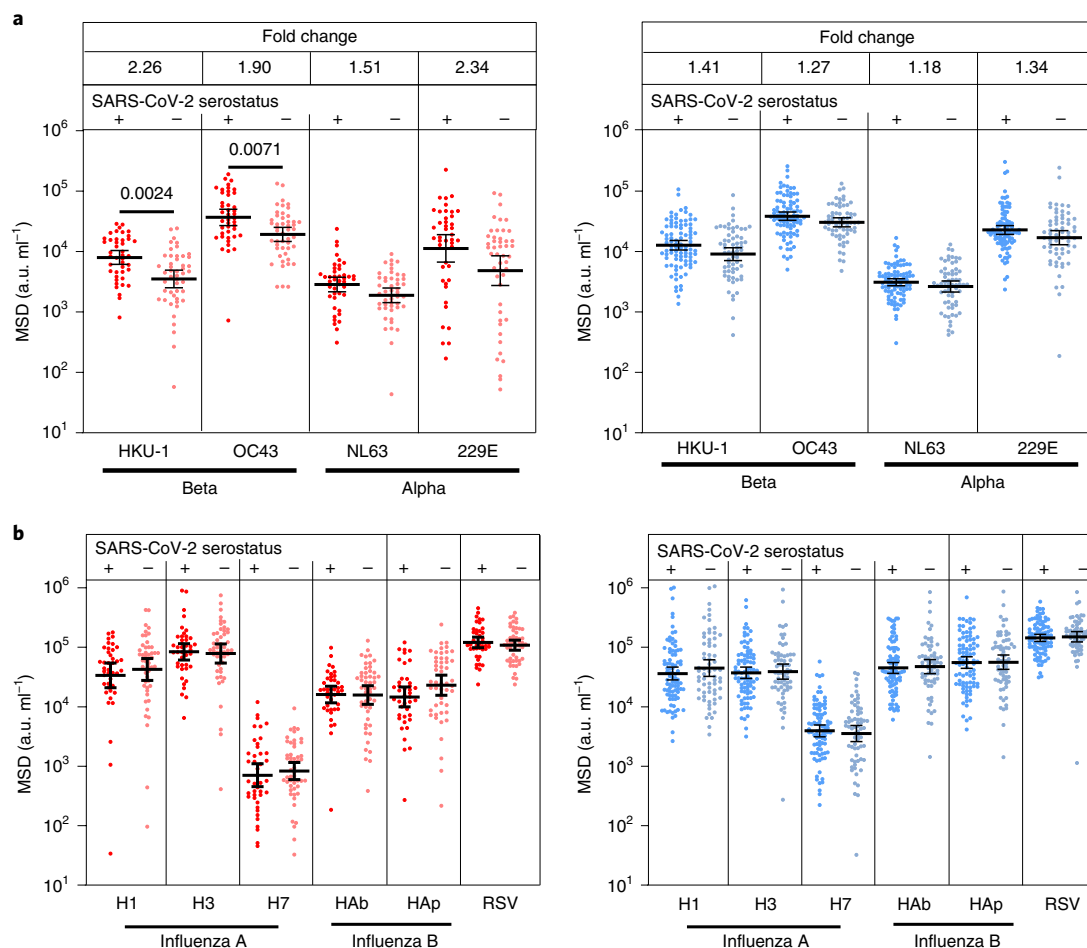


Fig. 2 | Antibody responses to hCoVs are back-boosted by SARS-CoV-2 in children. **a, b**, Antibody titers to the seasonal hCoV coronaviruses (**a**) and other respiratory viruses (**b**) in children (red) and adults (blue) based on SARS-CoV-2 serostatus (dark, seropositive; light, seronegative; seropositive/negative children $n = 43/48$, adults $n = 91/63$, respectively). Fold change indicates the difference between the GMTs in seropositive children and adults. The bars indicate the geometric mean with the 95% CI. Only significant differences are shown. Brown-Forsythe and Welch's ANOVA with Dunnett's T3 multiple comparison tests were used.

Samples were also obtained from 16 children who had seroconverted at least 12 months before the analysis. Antibody levels to spike and RBD were retained at a similar, although slightly reduced, level to those seen at 6 months while nucleocapsid-specific antibody levels were reduced ($P = 0.0004$) (Fig. 5c). Two of these 16 children (12.5%) had spike-specific antibody levels below the threshold while 4 children (25%) showed similar loss of nucleocapsid-specific antibodies, 1 of whom also lost the spike-specific response. Six of these donors had been analyzed previously at 6 months; matched individual comparisons revealed stable spike-specific antibody levels between 6 and 12 months postinfection whereas nucleocapsid-specific antibodies showed substantial waning, with 2 donors dropping below the cutoff (Fig. 5d).

Cellular immune responses were detectable in 84% of children and 79% of adults at least 6 months after infection. The magnitude of the spike-specific response was higher in children than in adults ($P = 0.032$) whereas responses to the N/M pool were seen in only 31% of children compared to 68% of adults (Fig. 5e,f). Fifteen children who had seroconverted over 12 months previously were also assessed by ELISpot. Compared to the cohort analysis at 6 months, T cell responses to spike were retained but somewhat reduced, while nucleocapsid-specific responses, although of lower magnitude, were retained at a similar level (Fig. 5g). Matched samples at 6 and 12 months were available for 5 of these children and were stable. These

data show that children broadly retained both antibody and cellular responses for extended periods after primary infection (Fig. 5h).

Enhanced binding but equal neutralization of variants of concern in children. SARS-CoV-2 variants of concern (VOC) may be able to partially escape immunity generated by previous infection or vaccination^{17,18}. Given the development and maintenance of cross-reactive high-level antibody responses in children, we assessed their relative recognition of spike protein from VOC. Plasma samples from 19 children and 18 adults at >6 months after primary infection were tested for binding to spike and RBD from Alpha (B.1.1.7), Beta (B.1.351) and Gamma (P.1) variants compared to the original Wuhan genotype, which was used in previous assays.

As described above, children, compared to adults, maintained higher levels of antibody binding to Wuhan spike (Figs. 5a and 6a) and this was also observed in binding to spike from the 3 VOC with 1.7, 1.8 and 2.1-fold higher geometric mean titers (GMTs) against Alpha, Beta and Gamma variants, respectively (Fig. 6a). Children also demonstrated higher binding to the RBD region of the 3 VOC, compared to adults, with 2.1, 1.8 and 2.9-fold higher GMTs, respectively ($P = 0.029$ and $P = 0.0114$ against Beta and Gamma, respectively; Kruskal-Wallis test with Dunn's multiple comparison test). Applying the threshold determined in earlier assays, 16 out of 19 (84%) children retained seropositive status to

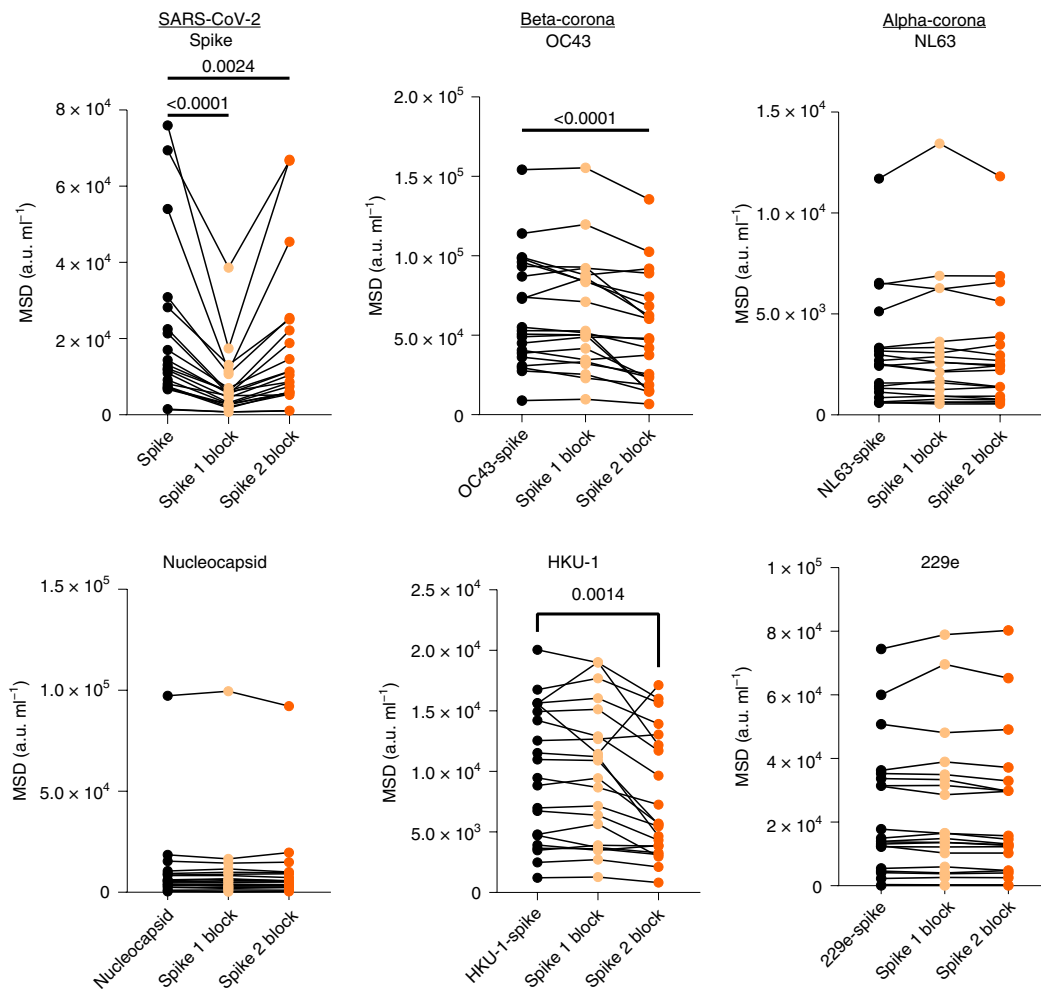


Fig. 3 | SARS-CoV-2 S2 domain antibodies cross-react with hCoV. Plasma from SARS-CoV-2 seropositive children ($n=21$) was assessed for binding to the spike protein of the 4 hCoVs or the spike or nucleocapsid regions of SARS-CoV-2. Plasma was either applied neat (control) or after preabsorption with either recombinant spike S1 domain (spike 1 block) or spike S2 domain (spike 2 block). S1 preabsorption markedly reduced binding to SARS-CoV-2 spike with no effect on hCoV, while S2 preabsorption reduced binding to OC43 and HKU-1. One-way repeated measures ANOVA with Holm-Sidak's multiple comparison test or Friedman test with Dunn's multiple comparisons test were used as appropriate.

both Beta and Gamma compared to only 5 out of 18 (28%) and 8 out of 18 (44%) of adults, respectively (Fig. 6b). Similar ratios of relative binding or inhibition of spike-angiotensin-converting enzyme 2 (ACE2) engagement with spike from Wuhan or VOC were seen in children and adults (Extended Data Fig. 3a,b and Supplementary Table 3), indicating that enhanced antibody binding to VOC is a function of overall quantitatively superior antibody responses in children.

We next assessed the ability of sera from children and adults to neutralize infection by live virus. Serum from adults showed markedly reduced capacity to neutralize the VOC and this was particularly noteworthy for B.1.351 (Fig. 6c,d). This pattern was also seen in children and no difference was seen in either maximal or 50% neutralization titer between adults and children. A similar profile was seen with a pseudotype-based neutralization assay (Extended Data Fig. 3d).

These data show that children developed higher antibody binding to SARS-CoV-2 VOC after natural infection compared to adults but displayed similar neutralizing ability.

Discussion

Age is the primary determinant of the clinical severity of SARS-CoV-2 infection and a life course assessment of virus-specific immunity

is essential to understand disease pathogenesis and design vaccine strategies in children. Our detailed analysis of adaptive immune memory identifies a number of important features in young children. A key finding was that the magnitude of the adaptive immune response to SARS-CoV-2 is higher in children compared to adults. This is somewhat different to previous reports that showed lower T cell responses in children⁶. This may reflect differences in assay systems since we used separate spike and N/M peptide pools to demonstrate the heightened spike-specific response. It has also been reported that children do not mount effective antibody responses against nucleocapsid in the early postinfection period^{3,5}. Using the well-validated MSD system, we observed nucleocapsid-specific antibody responses in children but it was noteworthy that immune responses were much more focused against spike¹⁹. Nucleocapsid is an abundant protein within the SARS-CoV-2 virion and it is possible that the magnitude of the N-specific response is a reflection of peak or aggregate viral load. The levels of virus within the upper airways at the time of primary infection are equivalent in children and adults²⁰ but relative changes over the course of infection are not known. Enhanced innate immune responses in children may also play an important role in limiting systemic replication and may explain the higher rates of asymptomatic and mild illness in children compared to adults²¹. Antibody levels generally correlated with

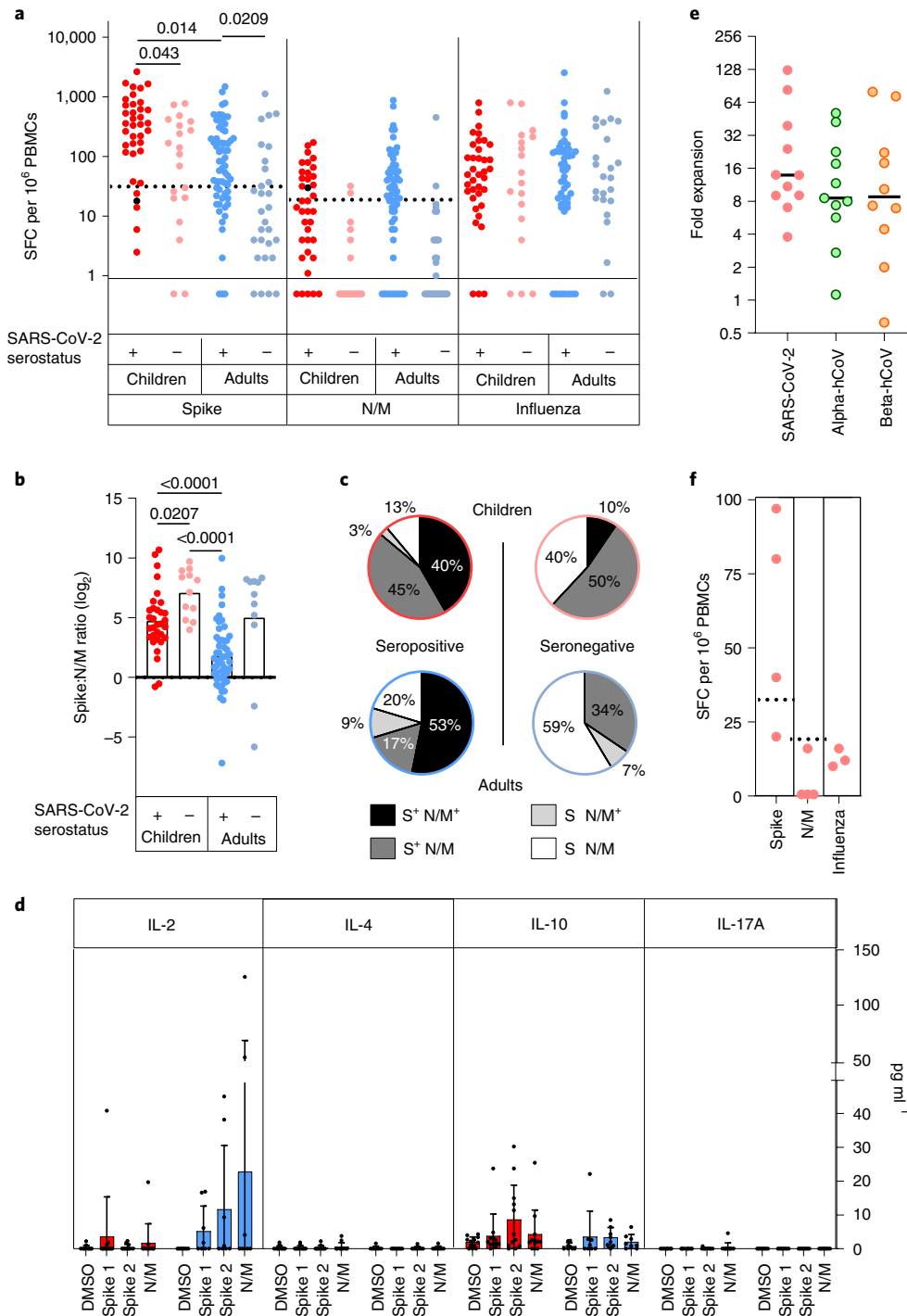


Fig. 4 | Spike-specific T cell responses in SARS-CoV-2 seropositive and seronegative children. **a**, SARS-CoV-2-specific T cell responses in children ($n=57$, red) and adults ($n=83$, blue) based on SARS-CoV-2 serostatus (dark; seropositive, light; seronegative). SARS-CoV-2 serostatus was 37/20 seropositive or negative in children and 64/29 seropositive or negative in adults, respectively. The assay used IFN- γ ELISpot using pepmixes containing overlapping peptides to spike, N/M or influenza and is shown in relation to serostatus. **b**, The magnitude of the spike-specific cellular response was compared to that against N/M and displayed as a ratio in seropositive and seronegative adults and children, as indicated. The bars indicate the mean. Brown-Forsythe and Welch's ANOVA with Dunnett's T3 multiple comparisons tests were used. **c**, Proportions of individuals within each cohort who demonstrated a cellular response to S or N/M peptides from SARS-CoV-2. **d**, Cytokine concentration within supernatants from the ELISpot cultures ($n=12$ children, red; $n=8$ adults, blue). The bars indicate the mean \pm s.d. **e**, hCoV-specific cellular responses showed equivalent expansion after stimulation of PBMCs from SARS-CoV-2 seronegative children with the SARS-CoV-2 S2 domain pepmix ($n=11$). Cultures were stimulated for 9 d and then assessed by IFN- γ ELISpot to the pepmix of the S2 domain from SARS-CoV-2 or the Alpha (OC43 and HKU-1) or Beta (NL63 and 229E) hCoV. Expansion is shown relative to unstimulated control cultures. The lines indicate the median. **f**, SARS-CoV-2-specific T cell response in PBMC samples taken from children before the COVID-19 pandemic ($n=4$). Dotted lines in **a** and **f** indicate pre-defined positive thresholds.

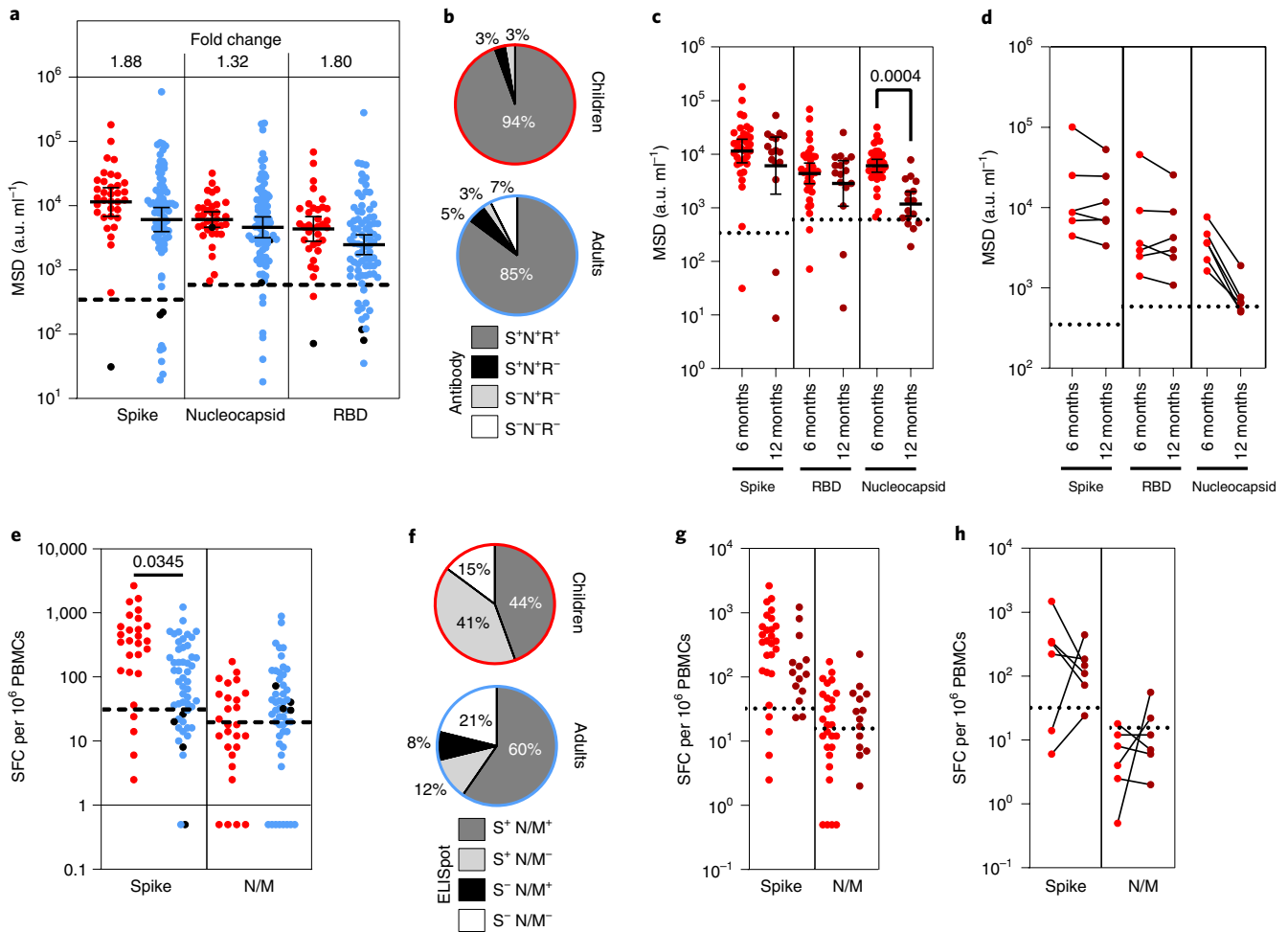


Fig. 5 | Immune responses are maintained in children at least six months after infection. **a**, Antibody responses in children ($n = 35$, red) and adults ($n = 81$, blue) who were seropositive at first testing and therefore at least 6 months post-primary infection. The bars indicate the GMT \pm 95% CI. The dotted lines indicate seropositive cutoffs. Fold change indicates increment in children's GMT compared to adults. The black dots indicate individuals who were seronegative for spike but retained a nucleocapsid-specific antibody response. **b**, Proportion of individuals retaining antibody responses to spike, nucleocapsid or RBD at ≥ 6 months. **c**, Antibody binding to spike, RBD or nucleocapsid in children ≥ 6 months ($n = 35$, red) or ≥ 12 months ($n = 16$, dark red) after infection. The bars indicate the GMT \pm 95% CI. The dotted lines indicate seropositive cutoffs. A one-way Kruskal-Wallis with Dunn's multiple comparisons test was used. **d**, Paired antibody levels for children ($n = 6$) at ≥ 6 and ≥ 12 months post-primary infection. The dotted lines indicate positive cutoffs. **e**, Spike-specific IFN- γ ELISpot in children ($n = 27$, red) and adults ($n = 52$, blue). The black dots indicate individuals who lacked a spike-specific response but retained a nucleocapsid-specific response. Brown-Forsythe and Welch's ANOVA with Dunnett's T3 multiple comparisons tests were used. SFC, spot-forming cell. **f**, Proportion of each cohort scored as responding to SARS-CoV-2 by ELISpot. **g**, Spike-specific IFN- γ ELISpot in children ≥ 6 months ($n = 27$, red) or ≥ 12 months ($n = 14$, dark red) after infection. The dotted lines indicate seropositive cutoffs. **h**, Paired ELISpot results for children at ≥ 6 and ≥ 12 months post-primary infection ($n = 6$). The dotted lines indicate seropositive cutoffs.

disease severity but none of the children or adults in this study suffered from severe disease or needed hospital admission.

One striking feature was that SARS-CoV-2 infection in children doubled antibody titers against all four Alpha and Beta hCoV subtypes. This pattern was not seen in adults where increased humoral responses were modest^{22,23}. Of note, increased antibody titers against hCoVs have also been observed after SARS-CoV-1 infection²⁴. Using protein domain preabsorption, we found that most of this response resulted from SARS-CoV-2-specific humoral responses that cross-reacted with the S2 domain of the two more closely related Beta-coronaviruses. The S2 domain is more highly conserved between hCoVs than S1 and this pattern is compatible with preferential targeting of structurally conserved epitopes by hCoV-specific antibodies in children²⁵ with the potential for neutralizing activity against SARS-CoV-2 (refs. 15,26). However, SARS-CoV-2 infection in children also boosted hCoV-specific antibody responses that

were not directly cross-reactive, as demonstrated by increased titers against Alpha-coronaviruses that could not be preabsorbed (Fig. 7). This may potentially reflect weakly cross-reactive B cell clones, potentially activated through T cell cross-recognition and is reminiscent of antibody boosting against H3 hemagglutinin after H1N1 infection in children with previous H3N2 infection²⁷. We found that titers of hCoV-specific antibodies were lower in seronegative children compared to adults but these are likely to increase after primary infection during the late teenage years^{13,25}; it appears that repeated infections may hone S1 domain-specific responses and lead to loss of cross-reactive S2-specific responses in adulthood¹⁵. Our data show that SARS-CoV-2 infection acts to fill the CoV-specific antibody space, producing antibodies against all coronaviruses and potentially supporting immunity in later life.

The development of antibodies against Alpha-coronaviruses that are not absorbed by the S2 domain of SARS-CoV-2 suggests

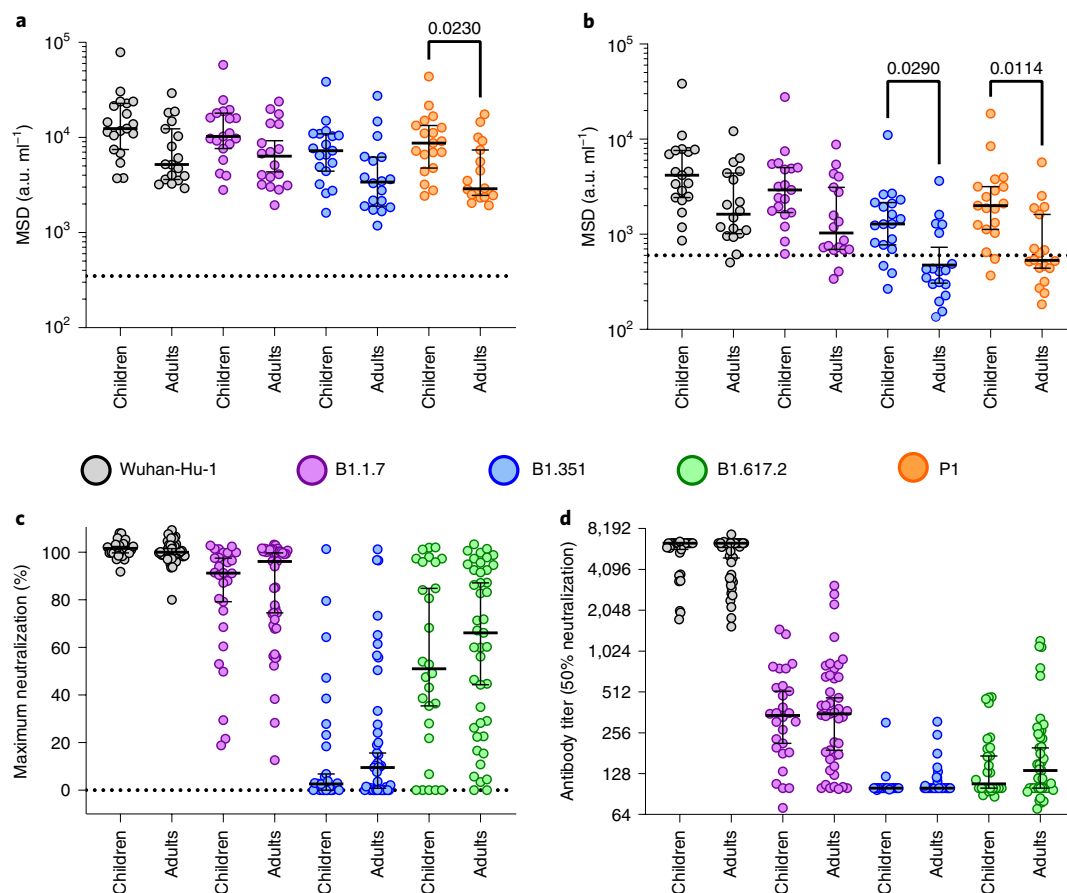


Fig. 6 | Superior antibody binding of SARS-CoV-2 variants in children and comparable neutralization. **a, b**, Antibody binding to spike (**a**) and RBD proteins (**b**) from SARS-CoV-2 variants using plasma from children ($n=19$) or adults ($n=18$). The bars indicate the geometric mean \pm 95% CI. Kruskal-Wallis with Dunn's multiple comparisons tests were used. **c, d**, Live virus neutralization assays on SARS-CoV-2 variants displayed as maximal neutralization of infection (**c**) and titer at 50% neutralization (**d**) using plasma from children ($n=28$) or adults ($n=43$). The bars indicate the median \pm 95% CI.

that there may be a lower affinity threshold for boosting related to heterologous immune responses in children, which might potentially represent an evolutionary adaptation to expand the memory pool early in life. It is interesting to speculate whether this may provide insight into the pathophysiology of PIMS-TS/MIS-C, where B cell activation drives a hyperinflammatory syndrome. Lack of pre-existing immunity to hCoV is a risk factor for PIMS-TS/MIS-C and may indicate a protective influence from a previous cross-reactive memory B cell pool⁸. Furthermore, the pathogenic antibodies associated with this condition are enriched for antibodies against heterologous pathogens and inflammation may result from Fc receptor-mediated monocyte activation²⁸.

This profile of an enhanced and cross-reactive humoral immune response in children was also apparent in the analysis of the cellular response to SARS-CoV-2. We found that the virus-specific T cell response was higher in children compared to adults and this mirrored the humoral response in that responses against the spike protein were markedly increased compared to nucleocapsid and envelope proteins. Virus-specific T cell responses in children also showed a differential cytokine response with markedly reduced production of IL-2. This may suggest a more highly differentiated profile in children compared to adults, which is in line with the enhanced magnitude of the response. Indeed, the spike-specific CD8⁺ T cell pool in children at 6 months after primary infection was dominated by an IL-2-IFN- γ ⁺TNF⁺ phenotype. As such, further long-term characterization of the T cell response in children, and the potential mechanisms that may act to drive T cell activation, are required.

We also observed that cross-reactive CoV-specific T cells are present in many children, both before and after SARS-CoV-2 infection. SARS-CoV-2-specific T cell responses were detectable in more than half of seronegative children, including samples taken pre-pandemic, and are likely to represent hCoV-specific T cell responses that cross-react against SARS-CoV-2 peptides^{29,30}. Of note, young adults were recently reported to have higher T cell responses to hCoV than older people and these can cross-react with SARS-CoV-2 (ref. ³¹). SARS-CoV-2-reactive T cells were also seen in some seronegative adults and it is also possible that some of these responses represent genuine SARS-CoV-2-specific T cells that have been generated after virus exposure in the absence of antibody seroconversion. This pattern has been reported in health care workers with high levels of viral exposure³² and it is possible that such conditions are also seen in primary schools where enforcement of social distancing is challenging.

It is tempting to speculate that this profile of cross-reactive antibody and cellular responses in children contributes to the excellent clinical outcomes in this group. In this regard, it would be interesting to assess matched pediatric samples from before and after SARS-CoV-2 infection to determine the relative contribution of cross-reactive hCoV-specific clones to the protective adaptive immune response.

Many participants were seropositive 6 months before the analysis and our data extend previous findings in adults^{33,34} to show sustained immunity over this time period. Moreover, we also found that children maintained higher antibody and cellular immune

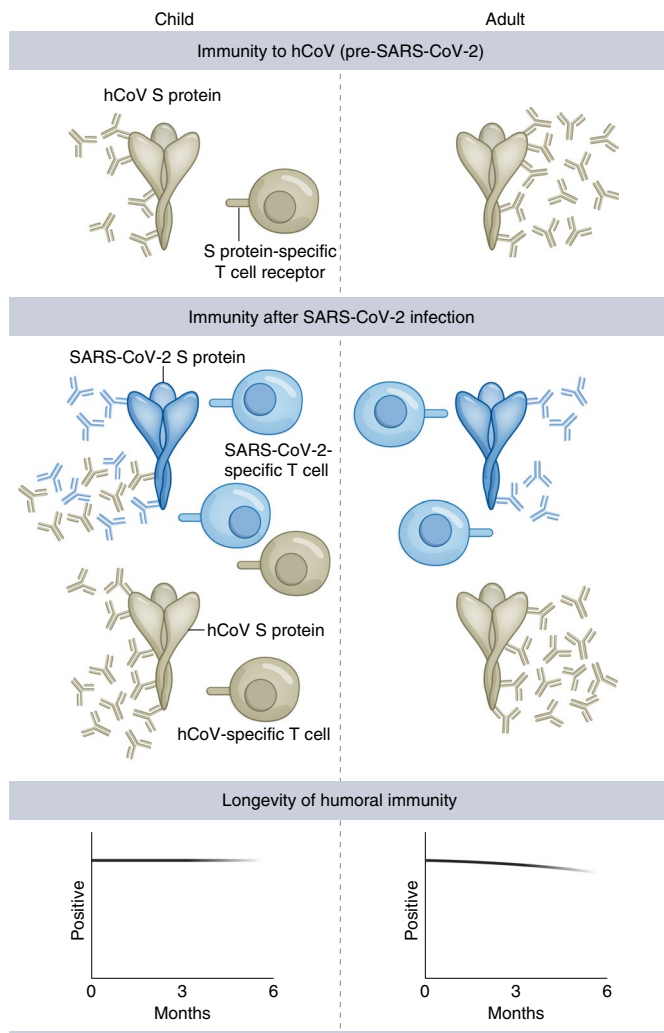


Fig. 7 | Model of adaptive immunity to coronaviruses in children and adults. Children develop hCoV spike S2-specific antibodies and cellular responses that can cross-react with SARS-CoV-2. Robust S1-specific adaptive responses develop after SARS-CoV-2 infection. Cross-reactive S2-specific responses probably contribute to immune control in children.

responses at this time point compared to adults with no loss of humoral response compared to loss in 7% of adults. There is increasing confidence in the relative stability of SARS-CoV-2-specific memory B cell and antibody responses but studies of antibody waning after natural infection are now difficult to perform in adults due to the widespread adoption of COVID-19 vaccines. Spike-specific antibody responses were also largely maintained in children at 12 months, whereas responses against nucleocapsid showed waning. T cell responses were broadly stable; it is important to consider that ELISpot analysis will only detect effector populations and a long-term memory subset is likely to have been established by this point. We could not compare 12-month values to the adult population because this latter group had undergone COVID-19 vaccination before this time point.

We also found that children possessed enhanced binding of antibodies to spike and RBD from viral VOC¹⁸. However, levels of neutralizing antibodies in live and pseudo-virus neutralization assays were comparable between adults and children. This suggests that children and adults develop comparable neutralizing antibody responses against the spike S1 domain but the increased antibody response in children results from antibodies targeting

non-neutralizing epitopes within S1 and S2. These antibodies could still have important effector potential through mechanisms such as antibody-directed cell cytotoxicity; further studies to examine the specificity and function of the SARS-CoV-2 B cell repertoire in children after natural infection or vaccination would be of value. In the light of the concern that SARS-CoV-2 will become an endemic infection³⁵, these findings augur well for immunity generated in childhood providing robust and sustained protection, including to emerging VOC.

In conclusion, we showed that children display a characteristically robust and sustained adaptive immune response against SARS-CoV-2 with substantial cross-reactivity against other hCoVs. This is likely to contribute to the relative clinical protection in this age group but these findings may also provide insight into the characteristic immunopathology that may develop. Furthermore, they will help to guide the introduction and interpretation of vaccine deployment in the pediatric population.

Online content

Any methods, additional references, Nature Research reporting summaries, source data, extended data, supplementary information, acknowledgements, peer review information; details of author contributions and competing interests; and statements of data and code availability are available at <https://doi.org/10.1038/s41590-021-01089-8>.

Received: 28 April 2021; Accepted: 3 November 2021;
Published online: 22 December 2021

References

- Booth, A. et al. Population risk factors for severe disease and mortality in COVID-19: a global systematic review and meta-analysis. *PLoS ONE* **16**, e0247461 (2021).
- Viner, R. M. et al. Susceptibility to SARS-CoV-2 infection among children and adolescents compared with adults: a systematic review and meta-analysis. *JAMA Pediatr.* **175**, 143–156 (2021).
- Weisberg, S. P. et al. Distinct antibody responses to SARS-CoV-2 in children and adults across the COVID-19 clinical spectrum. *Nat. Immunol.* **22**, 25–31 (2021).
- Pierce, C. A. et al. Immune responses to SARS-CoV-2 infection in hospitalized pediatric and adult patients. *Sci. Transl. Med.* **12**, eabd5487 (2020).
- Tosif, S. et al. Immune responses to SARS-CoV-2 in three children of parents with symptomatic COVID-19. *Nat. Commun.* **11**, 5703 (2020).
- Cohen, C. A. et al. SARS-CoV-2 specific T cell responses are lower in children and increase with age and time after infection. *Nat. Commun.* **12**, 4678 (2021).
- Flood, J. et al. Paediatric multisystem inflammatory syndrome temporally associated with SARS-CoV-2 (PIMS-TS): prospective, national surveillance, United Kingdom and Ireland, 2020. *Lancet Reg. Health Eur.* **3**, 100075 (2021).
- Consiglio, C. R. et al. The immunology of multisystem inflammatory syndrome in children with COVID-19. *Cell* **183**, 968–981.e7 (2020).
- Hoang, A. et al. COVID-19 in 7780 pediatric patients: a systematic review. *EClinicalMedicine* **24**, 100433 (2020).
- Gruber, C. N. et al. Mapping systemic inflammation and antibody responses in multisystem inflammatory syndrome in children (MIS-C). *Cell* **183**, 982–995.e14 (2020).
- Protein BLAST (National Center for Biotechnology Information, 2021); https://blast.ncbi.nlm.nih.gov/Blast.cgi?PROGRAM=blastp&PAGE_TYPE=BlastSearch&LINK_LOC=blasthome
- Dijkman, R. et al. Human coronavirus NL63 and 229E seroconversion in children. *J. Clin. Microbiol.* **46**, 2368–2373 (2008).
- Huang, A. T. et al. A systematic review of antibody mediated immunity to coronaviruses: kinetics, correlates of protection, and association with severity. *Nat. Commun.* **11**, 4704 (2020).
- Dijkman, R. et al. The dominance of human coronavirus OC43 and NL63 infections in infants. *J. Clin. Virol.* **53**, 135–139 (2012).
- Ng, K. W. et al. Preexisting and de novo humoral immunity to SARS-CoV-2 in humans. *Science* **370**, 1339–1343 (2020).
- Ladhani, S. N. et al. SARS-CoV-2 infection and transmission in primary schools in England in June–December, 2020 (sKIDs): an active, prospective surveillance study. *Lancet Child Adolesc. Health* **5**, 417–427 (2021).
- Sabino, E. C. et al. Resurgence of COVID-19 in Manaus, Brazil, despite high seroprevalence. *Lancet* **397**, 452–455 (2021).

18. Bates, T. A. et al. Neutralization of SARS-CoV-2 variants by convalescent and BNT162b2 vaccinated serum. *Nat. Commun.* **12**, 5135 (2021).
19. Ju, B. et al. Human neutralizing antibodies elicited by SARS-CoV-2 infection. *Nature* **584**, 115–119 (2020).
20. Madera, S. et al. Nasopharyngeal SARS-CoV-2 viral loads in young children do not differ significantly from those in older children and adults. *Sci. Rep.* **11**, 3044 (2021).
21. Neeland, M. R. et al. Innate cell profiles during the acute and convalescent phase of SARS-CoV-2 infection in children. *Nat. Commun.* **12**, 1084 (2021).
22. Anderson, E. M. et al. Seasonal human coronavirus antibodies are boosted upon SARS-CoV-2 infection but not associated with protection. *Cell* **184**, 1858–1864.e10 (2021).
23. Westerhuis, B. M. et al. Severe COVID-19 patients display a back boost of seasonal coronavirus-specific antibodies. Preprint at <https://doi.org/10.1101/2020.10.10.20210070> (2020).
24. Chan, K. H. et al. Serological responses in patients with severe acute respiratory syndrome coronavirus infection and cross-reactivity with human coronaviruses 229E, OC43, and NL63. *Clin. Diagn. Lab. Immunol.* **12**, 1317–1321 (2005).
25. Khan, T. et al. Distinct antibody repertoires against endemic human coronaviruses in children and adults. *JCI Insight* **6**, e144499 (2021).
26. Shrock, E. et al. Viral epitope profiling of COVID-19 patients reveals cross-reactivity and correlates of severity. *Science* **370**, eabd4250 (2020).
27. Meade, P. et al. Influenza virus infection induces a narrow antibody response in children but a broad recall response in adults. *mBio* **11**, e03243-19 (2020).
28. Bartsch, Y. C. et al. Humoral signatures of protective and pathological SARS-CoV-2 infection in children. *Nat. Med.* **27**, 454–462 (2021).
29. Mateus, J. et al. Selective and cross-reactive SARS-CoV-2 T cell epitopes in unexposed humans. *Science* **370**, 89–94 (2020).
30. Nelde, A. et al. SARS-CoV-2-derived peptides define heterologous and COVID-19-induced T cell recognition. *Nat. Immunol.* **22**, 74–85 (2021).
31. Saletti, G. et al. Older adults lack SARS CoV-2 cross-reactive T lymphocytes directed to human coronaviruses OC43 and NL63. *Sci. Rep.* **10**, 21447 (2020).
32. Reynolds, C. J. et al. Discordant neutralizing antibody and T cell responses in asymptomatic and mild SARS-CoV-2 infection. *Sci. Immunol.* **5**, eabf3698 (2020).
33. Zuo, J. et al. Robust SARS-CoV-2-specific T-cell immunity is maintained at 6 months following primary infection. *Nat. Immunol.* **22**, 620–626 (2021).
34. Dan, J. M. et al. Immunological memory to SARS-CoV-2 assessed for up to 8 months after infection. *Science* **371**, eabf4063 (2021).
35. Shaman, J. & Galanti, M. Will SARS-CoV-2 become endemic? *Science* **370**, 527–529 (2020).

Publisher's note Springer Nature remains neutral with regard to jurisdictional claims in published maps and institutional affiliations.



Open Access This article is licensed under a Creative Commons Attribution 4.0 International License, which permits use, sharing, adaptation, distribution and reproduction in any medium or format, as long as you give appropriate credit to the original author(s) and the source, provide a link to the Creative Commons license, and indicate if changes were made. The images or other third party material in this article are included in the article's Creative Commons license, unless indicated otherwise in a credit line to the material. If material is not included in the article's Creative Commons license and your intended use is not permitted by statutory regulation or exceeds the permitted use, you will need to obtain permission directly from the copyright holder. To view a copy of this license, visit <http://creativecommons.org/licenses/by/4.0/>.

© The Author(s) 2021

Methods

Sample collection. Public Health England (PHE) initiated prospective SARS-CoV-2 surveillance in primary schools across the UK after they reopened following the easing of national lockdown in June 2020. The protocol for sKIDs is available online (<https://www.gov.uk/guidance/covid-19-paediatric-surveillance>)¹⁶. Surveillance consisted of 2 arms, one involving weekly swabbing of primary school students and staff for SARS-CoV-2 infection (from June to mid-July 2020) and the other comprising swabbing and blood sampling taken in 3 rounds: beginning (1–19 June) and end (3–23 July) of the second half of the summer term when primary schools were partially reopened and after full reopening of all schools in September 2020, at the end of the autumn term (23 November–18 December). Samples for extended humoral and cellular analysis were taken in round 3. Additional samples from children found to be seropositive in round 1 were taken from 21 June to 24 July 2021. No statistical methods were used to predetermine sample sizes. Researchers were blinded to the serostatus of donors before ELISpot and serological assessment.

For each known SARS-CoV-2 seropositive individual, an age-matched (nearest age in years for students, nearest ten years for teachers) and sex-matched participant also underwent blood sampling. In total 154 adults and 91 children had sufficient blood sample for serology and cellular responses (Table 1). Convalescent plasma samples were also available from 35 children aged 10–13 years with PCR-confirmed SARS-CoV-2 infection, taken a median of 6 months (range 2–12 months) after the PCR result, from the Born in Bradford study³⁶.

Prepandemic plasma and PBMCs were obtained from healthy children as part of an ethically approved study (TriCICL) (South of Birmingham Research Ethics Committee 17/WM/0453, Integrated Research Application System 233593). Ethical review for the current study was provided by the PHE Research Ethics and Governance Group (PHE R&D REGG ref. no. NR0209). Written informed consent was obtained from all adult participants and from parents or guardians.

PBMC and plasma preparation. Blood tubes were spun at 300g for 10 min before removal of plasma, which was then spun again at 800g for 10 min and stored at –80 °C. The remaining blood was diluted 1:1 with Roswell Park Memorial Institute (RPMI) medium and PBMCs were isolated on a SepMate (STEMCELL Technologies) density centrifugation tube, washed with RPMI and rested in RPMI + 10% FCS overnight at 37 °C.

MSD serology assay. Quantitative immunoglobulin G (IgG) antibody titers were measured against trimeric spike protein, nucleocapsid and other coronavirus using the MSD V-PLEX COVID-19 Coronavirus Panel 2 (N05368-A1); Coronavirus Panel 7 (N05428A-1) responses to other respiratory viruses were measured using the MSD V-PLEX COVID-19 Respiratory Panel 1 (N05358-A1). Multiplex MSD assays were performed according to the manufacturer's instructions. Briefly 96-well plates were blocked. After washing, samples diluted 1:5,000 in diluent, as well as reference standard and internal controls, were added to the wells. After incubation plates were washed and detection antibody added. Plates were washed and were immediately read using a MESO TM QuickPlex SQ 120 system. Data were generated by Methodological Mind software v.4.0 and analyzed with the MSD Discovery Workbench v.4.0 software. Assay cutoffs with regard to prepandemic plasma samples from healthy donors are shown in Extended Data 1. Cutoffs used were 350 a.u. ml⁻¹ for spike, 600 a.u. ml⁻¹ for RBD and nucleocapsid and 15 a.u. ml⁻¹ for NTD.

Total IgG/A/M anti-spike SARS-CoV-2 ELISA. A total IgG/A/M anti-SARS-CoV-2 spike ELISA kit³⁷ was purchased from Binding Site. ELISA was performed according to the manufacturer's instructions. Optical density was compared to a known calibrator and expressed as a ratio to the calibrator. Samples with a ratio >1.0 were considered seropositive.

Cross-reactive antibody blocking. Plasma samples were prediluted 1:10 with PBS then preabsorbed by adding an equal volume of either recombinant spike S1 domain (catalog no. 10569-CV-100; R&D Systems) or spike S2 domain (catalog no. 10594-CV-100; R&D Systems) at a concentration of 500 µg ml⁻¹ in PBS or PBS alone (mock). Samples were incubated at 37 °C for 30 min. Samples were then diluted to a final dilution of 1:5,000 in MSD diluent and run on an MSD V-PLEX COVID-19 Respiratory Panel 2 plate in duplicate.

RBD-ACE2 competitive binding assay. The concentration of antibodies that inhibited the interaction between RBD and ACE2 was measured using a SARS-CoV-2 neutralization assay (BioLegend) according to the manufacturer's instructions. Briefly, plasma or positive control antibody were preincubated with biotinylated-Fc-chimera-S1-RBD protein before adding bead-bound ACE2. Binding of RBD to ACE2 was then measured by adding streptavidin-phycoerythrin. Samples were run on a BD LSR II flow cytometer and analyzed using the LEGENDplex v.8.0 software (BioLegend). Results were related to a known RBD neutralizing antibody standard and displayed as ng ml⁻¹.

Live virus and pseudotype-based neutralization assays. The clinical isolates used in the study were provided by PHE and Imperial College London.

Table 1 | Demographics and serostatus of study participants

	<i>n</i>	Age in years, median (range)	Sex	Infection >6 months ^a
Adults				
All	154	40 (20–71)	19% Male 81% Female	–
Seropositive	91	39 (20–71)	18% Male 82% Female	81
Seronegative	63	43 (26–65)	21% Male 79% Female	–
Children				
All	91	7 (3–11)	52% Male 48% Female	–
Seropositive	43	8 (5–11)	67% Male 33% Female	35
Seronegative	48	7 (3–11)	53% Male 47% Female	–

^aSeropositive at first assessment (June 2020).

A549-ACE2-TMPRSS2 cells³⁸ were seeded at a cell density of 1 × 10⁴ per well in 96-well plates 24 h before inoculation. Serum was titrated starting at a 1:100 dilution. The specified virus was then incubated at a multiplicity of infection of 0.01 with the serum for 1 h before infection. All wells were performed in triplicate; 72 h later infection plates were fixed with 8% formaldehyde and stained with Coomassie brilliant blue dye for 30 min. Plates were washed and dried overnight before quantification using a Celigo Imaging Cytometer (Nexcelom Bioscience) to measure staining intensity. Percentage cell survival was assessed by comparing the intensity of the staining to uninfected wells.

HEK293, HEK293T and 293-ACE2 cells were maintained in DMEM supplemented with 10% FCS, 200 mM of L-glutamine, 100 µg ml⁻¹ streptomycin and 100 IU ml⁻¹ penicillin. HEK293T cells were transfected with the appropriate SARS-CoV-2 S gene expression vector in conjunction with lentiviral vectors p8.91 and pCSFLW using polyethylenimine (Polysciences). Human immunodeficiency virus (HIV) (SARS-CoV-2) pseudotype-containing supernatants were collected 48 h posttransfection, aliquoted and frozen at –80 °C before use. The SARS-CoV-2 spike glycoprotein expression constructs for Wuhan-Hu-1, B.1.351 (South Africa) and B.1.617.2 have been described elsewhere³⁹. Constructs bore the following mutations relative to the Wuhan-Hu-1 sequence (GenBank ID: MN908947): B.1.351—D80A, D215G, L241–243del, K417N, E484K, N501Y, D614G and A701V; B.1.617.2—T19R, G142D, E156del, F157del, R158G, L452R, T478K, D614G, P681R and D950N. 293-ACE2 target cells were maintained in complete DMEM supplemented with 2 µg ml⁻¹ puromycin.

Neutralizing activity in each sample was measured by a serial dilution approach. Each sample was serially diluted in triplicate from 1:50 to 1:36,450 in complete DMEM before incubation with approximately 1 × 10⁶ counts per well of HIV (SARS-CoV-2) pseudotypes, incubated for 1 h and plated onto 293-ACE2 target cells. After 48–72 h, luciferase activity was quantified by adding Steadylyte Plus chemiluminescence substrate and analysis on a PerkinElmer EnSight multimode plate reader. Antibody titer was then estimated by interpolating the point at which infectivity had been reduced to 90% of the value for the no serum control samples.

Interferon-γ ELISpot. A pepmix pool containing 15-mer peptides overlapping by 10 amino acids from either the SARS-CoV-2 spike S1 or S2 domains and a combined pool of nucleoprotein and membrane and envelope were purchased from Alta Bioscience. Overlapping pepmixes from influenza A matrix protein 1, California/08/2009 (H1N1) (protein ID: C3W5Z8) and A/Aichi/2/1968 H3N2 (protein ID: Q67157) were purchased from JPT Peptide Technologies and combined as a relevant control.

T cell responses were measured using an interferon-γ (IFN-γ) ELISpot Pro Kit (Mabtech) as described previously³³. Briefly, fresh PBMCs were rested overnight before assay and 0.25–0.3 × 10⁶ PBMCs were added in duplicate per well containing either pepmix, anti-CD3 (positive) or dimethyl sulfoxide (DMSO) (negative) control. Samples were incubated for 16–18 h. The supernatant was collected and stored at –80 °C. Plates were developed according to the manufacturer's instructions and read using an AID plate reader (AID). Cutoff values were determined previously³³.

Cross-reactive T cell assay. A total of 1.3 × 10⁶ PBMCs were peptide-pulsed with SARS-CoV-2 S2 pepmix pool (JPT Peptide Technologies) at a concentration of 1 µg ml⁻¹ per peptide or an equal volume of DMSO. Cells were then plated into a 48-well plate and cultured in RPMI + 10% FCS + penicillin/streptomycin with the

addition of 20 U ml⁻¹ of IL-2 for 9 days, with frequent media changes. IL-2 was removed 24 h before the assay. Cells were washed and divided across four wells of an ELISpot plate and then restimulated with either SARS-CoV-2 S2 pepmix or S2 pepmixes from either the Beta (OC43 and HKU-1) or Alpha (NL63 and 229E) hCoVs. The results were read as for ELISpot and presented as expansion compared to the DMSO controls.

Cytokine measurement. Supernatants from donors with a detectable response in overnight ELISpot cultures were assessed using a LEGENDplex Th-profile 12-plex Kit (BioLegend) according to the manufacturer's instructions. Data were analyzed with the LEGENDplex v.8.0 software.

Intracellular cytokine staining. Cryopreserved PBMCs were thawed and rested overnight. Cells were then stimulated with a combined spike S1 and S2 peptide pool, at a final concentration of 1 µg ml⁻¹ per peptide or DMSO (mock). After 1 h, eBioscience protein transport inhibitor cocktail (Thermo Fisher Scientific) was added and cells were incubated for a further 5 h. eBioscience cell stimulation cocktail (Thermo Fisher Scientific) was used as a positive control. After stimulation, cells were washed (PBS + 0.1% BSA) and surface-stained at 4°C for 30 min. Cells were then washed and fixed in 2% paraformaldehyde. After washing, brilliant staining buffer (BD Bioscience) and a final concentration of 0.4% saponin were added. Cells were stained intracellularly at room temperature for 30 min. Cells were then washed and run on a BD FACSymphony A3 flow cytometer (BD Biosciences). Antibody details are provided in Supplementary Table 4.

Data visualization and statistics. Statistical tests, including normality tests, were performed as indicated using Prism 9 (GraphPad Software). Only significant results ($P < 0.05$) are displayed.

Reporting Summary. Further information on research design is available in the Nature Research Reporting Summary linked to this article.

Data availability

All data in this study are available within the article and its supplementary files and from the corresponding author upon reasonable request. Source data are provided with this paper.

References

36. Bird, P. K. et al. Growing up in Bradford: protocol for the age 7–11 follow up of the Born in Bradford birth cohort. *BMC Public Health* **19**, 939 (2019).
37. Cook, A. M. et al. Validation of a combined ELISA to detect IgG, IgA and IgM antibody responses to SARS-CoV-2 in mild or moderate non-hospitalised patients. *J. Immunol. Methods* **494**, 113046 (2021).
38. Rihn, S. J. et al. A plasmid DNA-launched SARS-CoV-2 reverse genetics system and coronavirus toolkit for COVID-19 research. *PLoS Biol.* **19**, e3001091 (2021).
39. Davis, C. et al. Reduced neutralisation of the Delta (B.1.617.2) SARS-CoV-2 variant of concern following vaccination. Preprint at <https://doi.org/10.1101/2021.06.23.21259327> (2021).

Acknowledgements

This work was partly funded by UK Research and Innovation (UKRI)/National Institute for Health Research through the UK Coronavirus Immunology Consortium

(P.M.). We acknowledge support from the G2P-UK National Virology Consortium (no. MR/W005611/1) funded by the UKRI (W.S.B., M.P.). The study was also funded in part by the Medical Research Council (no. MC UU 1201412, C.D., B.J.W.). We thank the staff, parents and especially the children at Addison Primary School, Avonmore Primary School, Beacon Primary, Canon Johnson CofE Primary, Carpenters Primary School, Cravenwood Primary, Curzon CofE Primary School, Didsbury CofE Primary, Ellen Wilkinson Primary School, Europa School UK, Hallsville Primary School, Hertsmere Jewish Primary School (Rimon), Highgate School, Kay Rowe Nursery School, Kilburn Grange, Little Eaton Primary School, London Fields (Hammersmith), Manor Primary School, Melcombe School, Milford Primary, Monega Primary School, Normand Croft School (Hammersmith), Park Primary School, Parochial CofE Primary and Nursery School, Portway Primary, Rimon Jewish Primary School (Rimon), Sandringham Primary School, Sacks Morasha Jewish Primary School (Rimon), Scott Wilkie Primary School, Selwyn Primary School, Shaftesbury Primary School, Southern Road Primary School, St Anne's CofE Lydgate Primary, St Edward's Catholic Primary School, St John's CofE Primary, St Mary's Catholic Primary School, St Paul's CofE Primary, St Peter's Smithills Dean CofE Primary School, St. Joseph's Primary, Unity Community Primary, Wolfson Hillel Primary School (Rimon) and Zaytouna Primary School for their participation in this study, without whom this work would not have been possible.

Author contributions

A.C.D., J.Z., P.M. and S.L. conceptualized the study. A.C.D., G. Tut, C.D., E.C.T., M.P. and B.J.W. devised the study methodology. A.C.D., G. Tut, C.D. and B.J.W. carried out the formal analysis. C.D., M.S.B., E.J., G.Tut, T.L., P.S., J. Begum., H.P., K.V., N.L., G.Tyson, E. Spalkova., S.M.-D. and J.Z. carried out the investigation. G.S.T., E. Syrimi., F.B., J. Beckmann., I.O.O., S.A., J.G., A.J.B., B.B., G.I., F.A., Z.A.-C., S.J., R. Borrow, E.L., J.W., R.A., D.W., W.S.B., J.P., G.A., K.E.B., M.E.R. and S.L. organized the resources. A.C.D., G.I. and J.Z. curated the data. A.C.D., P.M. and S.L. visualized the data. A.C.D., G. Tut, R. Bruton, J.W., D.W., C.D., E.C.T., M.P., B.J.W., J.Z., P.M. and S.L. supervised the study. R.Bruton, G.I., F.A., P.M. and S.L. managed the project. P.M., M.P., W.S.B. and S.L. acquired the funding. A.C.D., P.M. and S.L. wrote the original draft. All authors reviewed and edited the draft. These authors contributed equally: Megan S. Butler, Elizabeth Jinks, Gokhan Tut.

Competing interests

M.E.R. provided post-marketing surveillance reports on pneumococcal and meningococcal infection to vaccine manufacturers for which a cost recovery charge was made to GSK and Pfizer. The other authors declare no competing interests.

Additional information

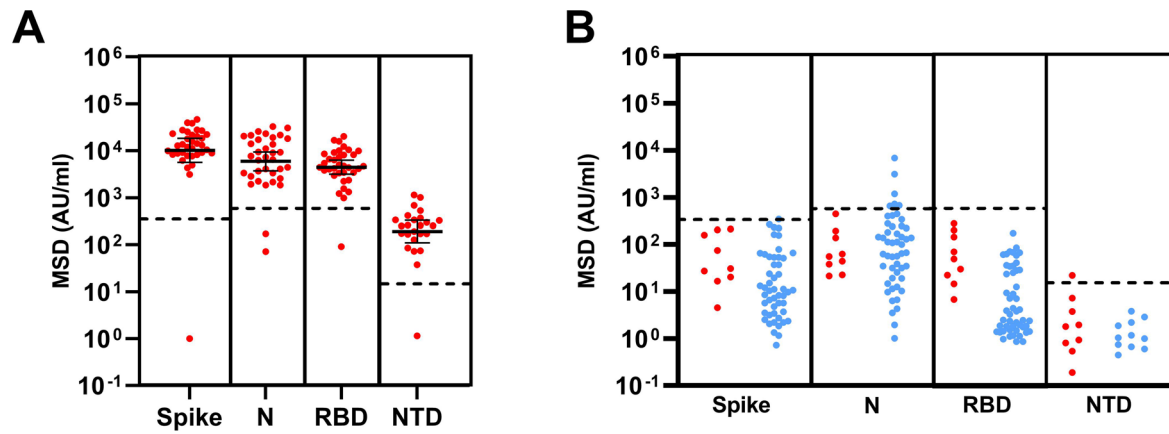
Extended data is available for this paper at <https://doi.org/10.1038/s41590-021-01089-8>.

Supplementary information The online version contains supplementary material available at <https://doi.org/10.1038/s41590-021-01089-8>.

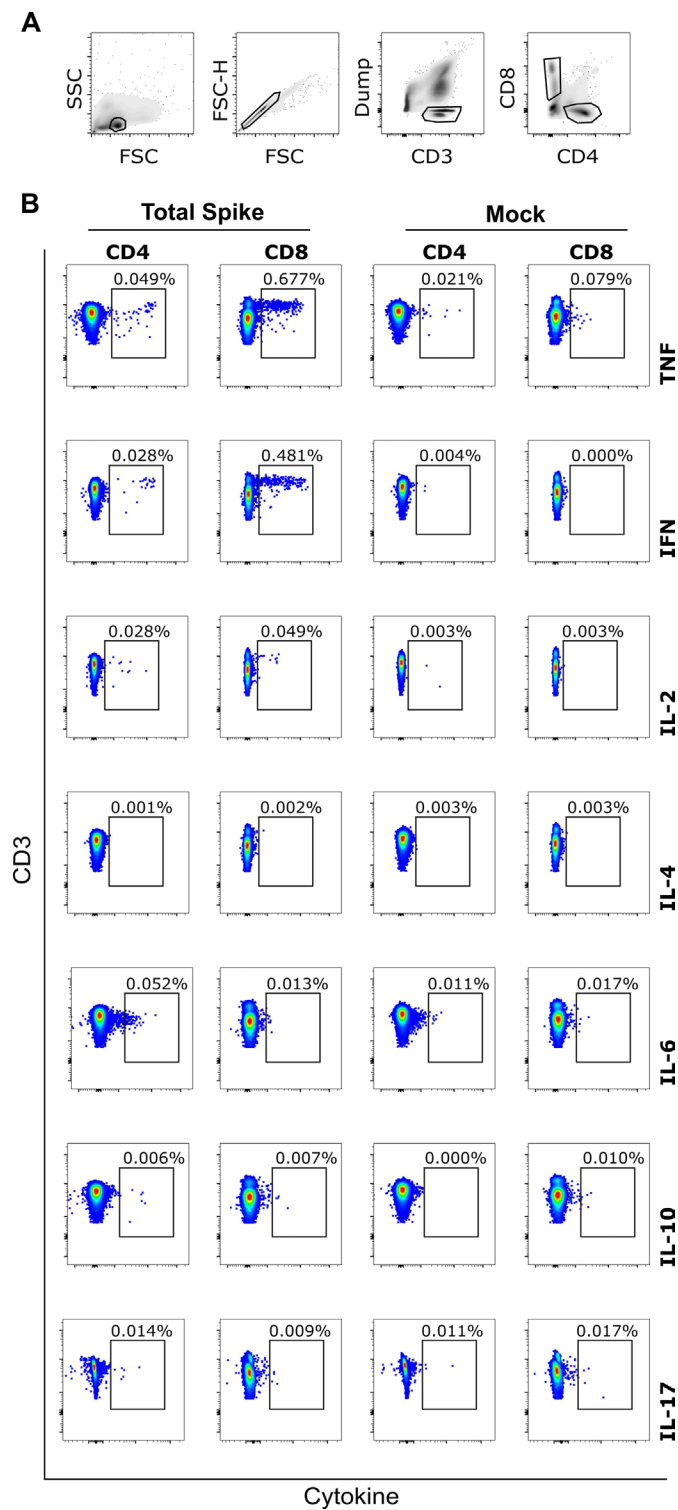
Correspondence and requests for materials should be addressed to Paul Moss.

Peer review information *Nature Immunology* thanks Jason Lavinder, Olivier Schwartz and the other, anonymous, reviewer(s) for their contribution to the peer review of this work. Peer reviewer reports are available. N. Bernard was the primary editor on this article and managed its editorial process and peer review in collaboration with the rest of the editorial team.

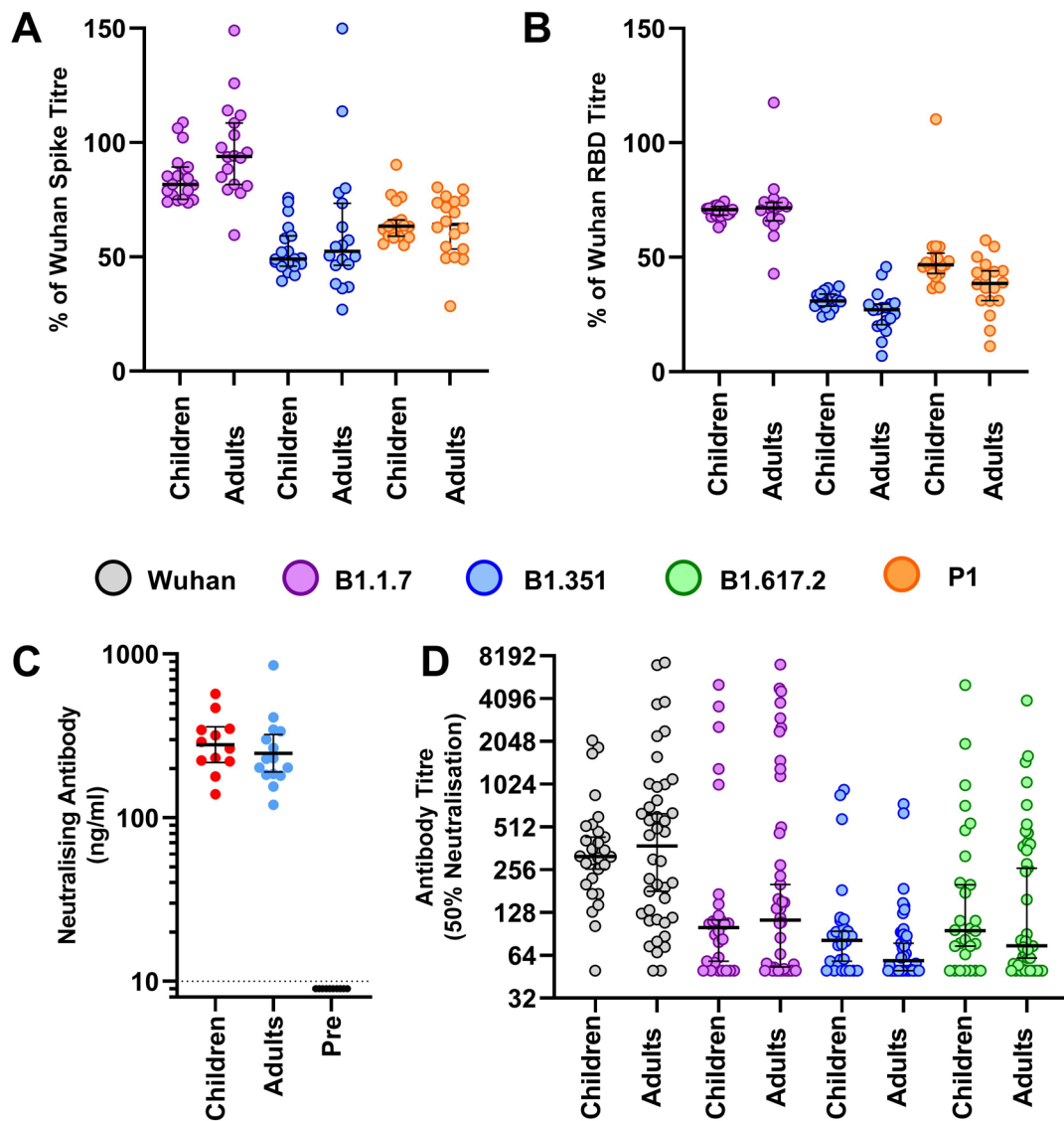
Reprints and permissions information is available at www.nature.com/reprints.



Extended Data Fig. 1 | MSD assay specificity and sensitivity. (a) MSD results using convalescent plasma samples from 35 children with PCR-confirmed SARS-CoV-2 infection. Bars indicate Geometric Mean \pm 95% CI. (b) Assay cut-offs were tested using plasma samples from nine children (red) and 50 adults (blue) taken prior to COVID-19. Dotted lines indicate the cut-off used.



Extended Data Fig. 2 | CD8+ T cells with a IL-2-TNF⁺IFN- γ ⁺ phenotype dominate the spike-specific T cell response in children. PBMC from SARS-CoV-2 seropositive children were stimulated for 6hrs in the presence of spike peptide pool and then cytokine production analysed by flow cytometry by intracellular cytokine staining (ICS). **(a)** Gating strategy for analysis. **(b)** Representative example of ICS staining from one child at six months post SARS-CoV-2 infection showing TNF + IFN- γ + CD8+ T cell response representing 0.48% of the global CD8+ T cell repertoire.



Extended Data Fig. 3 | Antibody binding, RBD-ACE2 inhibition and pseudo-neutralisation of SARS-CoV-2 VOC in plasma from children or adults. (a) Antibody titres normalised to the Wuhan sequence as determined by MSD to total spike and **(b)** RBD from VOC as indicated in children ($n=19$) and adults ($n=18$) ≥ 6 months post primary infection. Bars indicate Median \pm 95% CI. **(c)** Antibody inhibition in an RBD-ACE2 competitive binding assay using plasma ≥ 6 months post infection in children ($n=12$) and adults ($n=15$). Results from pre-pandemic adult samples are also shown ($n=10$). Bars indicate geometric mean \pm 95% CI. **(d)** Results from pseudo-virus neutralisation assays displayed as titre at 50% neutralisation from children ($n=28$) and adults ($n=43$) ≥ 6 months post primary infection. Bars indicate Median \pm 95% CI.

Reporting Summary

Nature Research wishes to improve the reproducibility of the work that we publish. This form provides structure for consistency and transparency in reporting. For further information on Nature Research policies, see our [Editorial Policies](#) and the [Editorial Policy Checklist](#).

Statistics

For all statistical analyses, confirm that the following items are present in the figure legend, table legend, main text, or Methods section.

n/a Confirmed

- The exact sample size (n) for each experimental group/condition, given as a discrete number and unit of measurement
- A statement on whether measurements were taken from distinct samples or whether the same sample was measured repeatedly
- The statistical test(s) used AND whether they are one- or two-sided
Only common tests should be described solely by name; describe more complex techniques in the Methods section.
- A description of all covariates tested
- A description of any assumptions or corrections, such as tests of normality and adjustment for multiple comparisons
- A full description of the statistical parameters including central tendency (e.g. means) or other basic estimates (e.g. regression coefficient) AND variation (e.g. standard deviation) or associated estimates of uncertainty (e.g. confidence intervals)
- For null hypothesis testing, the test statistic (e.g. F , t , r) with confidence intervals, effect sizes, degrees of freedom and P value noted
Give P values as exact values whenever suitable.
- For Bayesian analysis, information on the choice of priors and Markov chain Monte Carlo settings
- For hierarchical and complex designs, identification of the appropriate level for tests and full reporting of outcomes
- Estimates of effect sizes (e.g. Cohen's d , Pearson's r), indicating how they were calculated

Our web collection on [statistics for biologists](#) contains articles on many of the points above.

Software and code

Policy information about [availability of computer code](#)

Data collection Methodological Mind software; Meso Scale Diagnostics Workbench version 4, BD FACSDiva Version 9.0. AID ELISpot software version 8.

Data analysis Meso Scale Diagnostics Workbench version 4, Flow Jo Version 10.6.1, Graphpad Prism Version 9, Legendplex Software Version 8.

For manuscripts utilizing custom algorithms or software that are central to the research but not yet described in published literature, software must be made available to editors and reviewers. We strongly encourage code deposition in a community repository (e.g. GitHub). See the Nature Research [guidelines for submitting code & software](#) for further information.

Data

Policy information about [availability of data](#)

All manuscripts must include a [data availability statement](#). This statement should provide the following information, where applicable:

- Accession codes, unique identifiers, or web links for publicly available datasets
- A list of figures that have associated raw data
- A description of any restrictions on data availability

The data that support the findings of this study are available from the supporting data source files.

Field-specific reporting

Please select the one below that is the best fit for your research. If you are not sure, read the appropriate sections before making your selection.

Life sciences Behavioural & social sciences Ecological, evolutionary & environmental sciences

For a reference copy of the document with all sections, see [nature.com/documents/nr-reporting-summary-flat.pdf](https://www.nature.com/documents/nr-reporting-summary-flat.pdf)

Life sciences study design

All studies must disclose on these points even when the disclosure is negative.

Sample size	All Adult and Children found to be SARS-CoV-2 sero-positive in the prior SKIDS study were invited to participate further for this study, all donors willing to participate were included. Matched donors of a similar age who were previously sero-negative were also asked to participate.
Data exclusions	Donors were excluded from ELISpot for the following reasons, a) insufficient cell number, b) failure of positive control wells, c) high background in the negative control wells. Data were excluded from the cross-reactive spike blocking assay if a reduction of SARS-CoV-2 Spike antibody level was not evident. Data was excluded from MSD analysis if multiple spots failed to give signal to antigens of which response would be expected i.e. hCoV.
Replication	Due to the limitations of blood volume it was not possible to repeat cellular assays. Serological assays were assessed by multiple methods as stated.
Randomization	All donor were treated equally. Researchers were blinded to the serostatus of donors until initial MSD and ELISpot data acquisition had been completed.
Blinding	Researchers were blinded to the serostatus of donors until initial MSD and ELISpot data acquisition had been completed.

Reporting for specific materials, systems and methods

We require information from authors about some types of materials, experimental systems and methods used in many studies. Here, indicate whether each material, system or method listed is relevant to your study. If you are not sure if a list item applies to your research, read the appropriate section before selecting a response.

Materials & experimental systems

n/a	Involved in the study
<input type="checkbox"/>	<input checked="" type="checkbox"/> Antibodies
<input type="checkbox"/>	<input checked="" type="checkbox"/> Eukaryotic cell lines
<input checked="" type="checkbox"/>	<input type="checkbox"/> Palaeontology and archaeology
<input checked="" type="checkbox"/>	<input type="checkbox"/> Animals and other organisms
<input type="checkbox"/>	<input checked="" type="checkbox"/> Human research participants
<input checked="" type="checkbox"/>	<input type="checkbox"/> Clinical data
<input checked="" type="checkbox"/>	<input type="checkbox"/> Dual use research of concern

Methods

n/a	Involved in the study
<input checked="" type="checkbox"/>	<input type="checkbox"/> ChIP-seq
<input type="checkbox"/>	<input checked="" type="checkbox"/> Flow cytometry
<input checked="" type="checkbox"/>	<input type="checkbox"/> MRI-based neuroimaging

Antibodies

Antibodies used	CD14 clone HCD14 APC-Cy7 Biolegend cat 325620 lot B282904 CD19 clone HIB19 APC-Cy7 Biolegend cat 302218 lot B279663 CD3 clone UCHT1 Fitc Biolegend cat 300406 lot B279208 CD4 clone RPAT4 Per-CP-Cy5.5 Biolegend cat 300529 lot B277600 CD8 clone SK1 BV510 Biolegend cat 344732 lot B270694 IL-2 clone MQ117H12 Pe-Cy7 Biolegend cat 500326 lot B314085 IL-4 clone MP4 25D2 APC Biolegend cat 500813 lot B262980 IL-6 clone MQ2 13A5 PE-Dazzle 594 Biolegend cat 501122 lot B284858 IL-10 clone Jes3-9D7 PE Biolegend cat 501404 lot B285627 IL-17A clone BL168 BV421 Biolegend cat 512322 lot B317903 IFN γ clone 4S.B3 AF700 Biolegend cat 502520 lot B302043 TNF clone Ab11 BV711 Biolegend cat 502940 B326604
Validation	These antibodies and intracellular cytokine staining are standardly used. Citing references and application references, alongside example staining are provided at www.Biolegend.com . Cell lineage markers (i.e. CD14, CD19, CD3, CD4, CD8) were titrated alone or in combination using health donor PBMC, to obtain concentrations which clearly identified populations of interest, and ensure staining of the negative population was not present. Intracellular antibodies for this panel were titrated and tested on healthy donor

PBMC using PMA/Ionomycin and widely recognized peptide antigen (CEFX), cells were stimulated as described in methods, PMA stimulates cytokine production by T cells irrespective of antigen recognition, as such PBMC produce the cytokines listed (examples of PMA induced cytokine production for each of the antibodies can be found on the product page at www.biolegend.com). Following surface staining for the lineage markers previously optimised. Titration of the various antibodies was then preformed to determine the optimal dilution to provided resolution of cytokine producing cells, unstimulated cells were used to ensure specificity and absence of staining in the negative population. Examples of staining and gating are provided in Extended Data Figure 2. A positive control using PMA/Ionomycin was included in all experiments.

Eukaryotic cell lines

Policy information about [cell lines](#)

Cell line source(s)	HEK-293 were obtained circa 2000 from Yasu Takeuchi, University College London.
Authentication	HEK-293 have not been formally identified, but have been in the possession of Brian Willet and used by Brian Willet since 2000.
Mycoplasma contamination	All cell lines were routinely tested for mycoplasma and are negative.
Commonly misidentified lines (See ICLAC register)	Not on the registry.

Human research participants

Policy information about [studies involving human research participants](#)

Population characteristics	Previously sero-positive donors (Children aged 3-11 and adults aged 20-71) were age and gender matched as closely as possible, (maximally within 1yr for children, 10 yrs for adults). Age and gender for the sero-positive and negative cohorts are provided in table 1. Full characteristics of the sKIDS cohort are provided in the sKIDS study protocol and publication (https://www.gov.uk/guidance/covid-19-paediatric-surveillance , Ladhani, S.N. et al. SARS-CoV-2 infection and transmission in primary schools in England in June-December, 2020 (sKIDS): an active, prospective surveillance study. The Lancet. Child & adolescent health (2021)).
Recruitment	Adult and Children found to be SARS-CoV-2 sero-positive in the prior sKIDS study were invited to participate further for this study, only Sero-positive donors reporting mild or asymptomatic infection were included in the collection. All donors willing to participate were included. Matched donors of a similar age who were previously sero-negative were also asked to participate. These donors are the most relevant control group as such no bias should be evident.
Ethics oversight	Written informed consent was obtained from all donors, either directly from adults (aged >18 yrs old) or from legally authorized representatives of minor participants (age below <18 yrs old). Ethical approval was obtained from PHE Research Ethics Governance Group (reference NR0209; May 16, 2020), South of Birmingham Research Ethics Committee (REC: 17/WM/0453, IRAS: 233593), Bradford Research Ethics Committee (Ref 07/H1302/112).

Note that full information on the approval of the study protocol must also be provided in the manuscript.

Flow Cytometry

Plots

Confirm that:

- The axis labels state the marker and fluorochrome used (e.g. CD4-FITC).
- The axis scales are clearly visible. Include numbers along axes only for bottom left plot of group (a 'group' is an analysis of identical markers).
- All plots are contour plots with outliers or pseudocolor plots.
- A numerical value for number of cells or percentage (with statistics) is provided.

Methodology

Sample preparation	PBMC was prepared as described, excess cells were cryopreserved in 10%DMSO/90% FBS, and stored in the vapor phase of liquid nitrogen. Cells were thawed by warming at 37°C and washed in warmed media. Cells were rested overnight prior to experiment.
Instrument	28 color BD FACS Symphony A3 Flow cytometer.
Software	BD FACS Diva Version 9.
Cell population abundance	Cell sorting was not preformed, analysis by flow cytometry only. Observed cytokine producing cells in response to SARS-CoV-2 Spike peptide pool ranged from 0.677% of parent cell population (CD8 T cells) to >0.001%, dependent upon cytokine produced, response was determined against abundance in a DMSO stimulated negative control, as shown in Extended Data Figure 2.

Gating strategy

Lymphocytes were gated by FSC/SSC, followed by doublet exclusion by FSC-A/FSC-H. Live CD3+ CD14- CD19- cells were then gated, and CD4+CD8- or CD4-CD8+ T cells were finally gated.

Tick this box to confirm that a figure exemplifying the gating strategy is provided in the Supplementary Information.